Analyst

PAPER

View Article Online
View Journal | View Issue



Cite this: *Analyst*, 2026, **151**, 1332

# Untargeted mass spectrometry to investigate ocean acidification in *Cancer borealis* using optimized metabolite extraction methods

Yunxiao Yao, [a] Olga Riusech,[a] Shuling Xu [b] and Lingjun Li *[a,b,c,d]

Received 25th July 2025,
Accepted 27th January 2026

DOI: 10.1039/d5an00788g

rsc.li/analyst

Ocean acidification (OA) refers to the ongoing decline in ocean pH caused by the cascading effects of increased atmospheric $CO_2$, which has significant negative impacts on various marine organisms, particularly crustaceans with calcified shells. However, research on the metabolic responses of crustaceans remains limited. In this study, we performed untargeted metabolomics on hemolymph samples from *Cancer borealis* (Jonah crab), a crustacean species well known for its tolerance to temperature and pH changes, to investigate its metabolic responses to OA. Two extraction methods—isopropanol (IPA) and acidified methanol (AcMeOH)—were employed to capture a broad range of metabolites and small peptides. Both methods enabled comprehensive detection; however, IPA extraction yielded more consistent and extensive metabolite coverage, identifying 43 lipids compared to only 15 with AcMeOH. We identified 15 metabolites that responded significantly to OA. Several metabolites, including the potential neuropeptide cycloprolylglycine and the exogenous compound curcumin, exhibited concentration changes under OA exposure, suggesting their potential relevance in stress response pathways triggered by environmental stress. Overall, we highlight IPA as a more effective extraction method for untargeted metabolomics of crustacean hemolymph. Our study elucidates metabolic dynamics that enhance our understanding of the physiological adaptability of marine crustaceans under environmental stress and provides a comprehensive dataset for future OA research.



## Introduction

Ocean acidification (OA) refers to the systematic lowering of ocean pH caused by the absorption of atmospheric $CO_2$ into seawater. The increased partial pressure of atmospheric $CO_2$ drives more $CO_2$ into the oceans, where it reacts with water to form bicarbonate ions and hydrogen ions ($H^+$). This process ultimately reduces seawater carbonate ion concentrations and pH, while increasing bicarbonate ions. OA is a heterogeneous process that is exacerbated in regions with dense industrial runoff. In the Arctic, the decrease in seawater pH is intensified by a concurrent reduction in the buffering capacity of surface waters, driven by increased sea ice melt and greater inflow of Atlantic water carrying large amounts of anthropogenic $CO_2$ into the Arctic Ocean.[1–5] While the ocean's surface pH of 8.2 is widely accepted, projections suggest a decline of 0.3–0.4 pH units by the year 2100.[6] This decline is expected to result in thinning and acid erosion of calcium carbonate shells, as evidenced by studies using *Limacina helicina* pteropods as potential OA indicators.[7–9] In addition to pH changes, salinity, temperature, and nutrient availability are also expected to shift over the 21st century, impacting the health of marine species globally.[10–12]

Many marine species have been studied for their ability to withstand the effects of OA; however, calcifying organisms that build their shells and skeletons from calcite and/or aragonite forms of calcium carbonate ($CaCO_3$) remain a major concern due to the potential impact of acidified seawater on their calcification rates.[13–16] Studies have reported negative effects of OA on coral and bivalve species, including net shell dissolution, increased mortality, reduced tissue energy reserves, and impaired soft tissue growth under elevated $CO_2$ conditions.[16,17] In contrast, crustaceans appear to exhibit greater physiological tolerance to OA. Notably, *Callinectes sapidus* (blue crab), *Homarus americanus* (American lobster), and *Penaeus plebejus* (edible shrimp) have shown increased calcification rates, suggesting potential resistance to shell dissolution in acidified seawater.[16] However, OA has also been shown to impair crab foraging behaviour, leading to reduced

[a]*Department of Chemistry, University of Wisconsin, Madison, WI 53706, USA*
[b]*School of Pharmacy, University of Wisconsin, Madison, WI 53705, USA*
[c]*Lachman Institute for Pharmaceutical Development, School of Pharmacy, University of Wisconsin-Madison, Madison, WI 53705, USA*
[d]*Wisconsin Center for NanoBioSystems, School of Pharmacy, University of Wisconsin-Madison, Madison, WI 53705, USA. E-mail: lingjun.li@wisc.edu*

prey consumption, shorter handling times, and decreased duration of unsuccessful predation attempts.[18] Additionally, crab shell and claw integrity may deteriorate under OA, with blue crabs exhibiting reduced claw strength and weakened pinch force.[19]

Investigating how marine crustacean species withstand OA is of significant interest to researchers aiming to understand and predict metabolic adaptations, with the goal of anticipating potential biodiversity and economic consequences associated with global climate change. Despite this interest, research on the metabolic responses of crustaceans, including crabs, remains limited. To address this gap, mass spectrometry (MS) serves as a powerful analytical tool for comprehensive metabolic profiling, enabling the quantification of all ionizable compounds within a selected mass-to-charge ratio ($m/z$) range. Untargeted metabolomics is a robust approach for globally profiling small-molecule metabolites and investigating key metabolic pathways in biological samples without chemical derivatization or isotopic labelling.[20,21] Unlike targeted metabolomics, which quantifies a predefined set of known metabolites, untargeted approaches enable the discovery of unexpected or previously uncharacterized metabolic alterations.[22] However, the identification of small-molecule metabolites (<1500 Da) by MS remains challenging due to their vast chemical diversity, requiring tailored sample preparation strategies to effectively isolate molecules with different physicochemical properties. A widely used sample preparation strategy for broad-spectrum metabolite analysis is the dilute-and-shoot (DnS) approach, which typically involves metabolite extraction *via* protein precipitation (PPT) prior to liquid chromatography–tandem mass spectrometry (LC–MS/MS) analysis.[23]

Numerous PPT protocols have been developed for metabolomic analysis, each yielding distinct metabolic profiles. Here we explore two different PPT methods, isopropanol extraction and acidified methanol extraction, and compare their extraction profiles for small molecule metabolites. We further evaluate the metabolome coverage achieved by each extraction method. *Cancer borealis* (Jonah crab) is a model species well known for its ability to tolerate temperature and pH changes and has been extensively studied in peptidomics and nervous system research.[24–27] To better understand the biological pathways involved in Jonah crab's response to OA, we investigate its hemolymph metabolome under current pH conditions (pH 8.2) and projected future OA conditions (pH 7.8).

# Experimental

## Materials

Optima grade Methanol (MeOH), Optima grade glacial acetic acid, Optima grade acetonitrile (ACN), Optima grade IPA, and Optima grade water were purchased from Fisher Scientific (Pittsburgh, PA, USA). AcMeOH was prepared by combining MeOH, water, and glacial acetic acid at a 90 : 9 : 1 ratio. AcMeOH and IPA PPT solutions were stored on ice for at least 30 minutes prior to PPT extraction experiments.

## OA exposure experiments

Male *Cancer borealis* (Jonah crabs) were purchased from a local store (Global Market, Madison, WI, USA) and acclimated for one week in a recirculating seawater system (Aquaneering, California, USA) maintained at 30 ppt salinity under a 12 hours light/12 hours dark cycle. The OA exposure experiments were conducted following protocols previously established in our laboratory.[28] The crabs were starved for a week prior to experimentation to minimize dietary-derived interference. For OA exposure experiments (Fig. 1), crabs were exposed to either control (pH 8.2) or acidified seawater (pH 7.8, adjusted *via* $CO_2$ sparging) for 2 or 4 hours, with five biological replicates per group. The acidified seawater was simulated by introducing $CO_2$ gas. A pH sensor (American Marine Pinpoint pH Monitor) and a dissolved oxygen (D.O.) sensor (American Marine Pinpoint Oxygen Monitor) were placed at the corner of the tank farthest from the $CO_2$ gas tank tube. A moderate pH level (7.7–7.9) was achieved quickly by introducing $CO_2$ *via* gas tank into the housing tank. The air saturation was at 50%–60%, which was considered as moderate hypoxic condition. The pH level was stabilized before the stress experiment started. D.O. level and pH level were monitored throughout the experiment. Following treatment, animals were chilled on ice for 30 minutes before hemolymph extraction. Hemolymph (200 μL) was collected from each crab using a sterile syringe and immediately mixed with 200 μL of cold PPT solution (either IPA or AcMeOH). Crabs were subsequently returned to the tank for recovery. Samples were mixed on ice, incubated overnight at −20 °C, and centrifuged at 16 000*g* for 15 min at 4 °C. Supernatants were transferred to pre-weighed tubes, dried *via* vacuum centrifugation, and stored at −20 °C. Before LC-MS/MS analysis, dried extracts were reconstituted in 300 μL of 50 : 50 (v/v) optima-grade acetonitrile/water, vortexed, and centrifuged at 16 000*g* for 5 min at 4 °C to remove debris. The supernatants were transferred to LC-MS vials for analysis.

## LC-MS/MS data collection

An Agilent 1290 Infinity II HPLC system (Agilent Technologies, USA) equipped with a Kinetex 2.6 μm hydrophilic interaction liquid chromatography (HILIC) column (100 Å, 150 × 4.6 mm) was coupled to an Agilent 6560C quadrupole time-of-flight (Q-TOF) mass spectrometer. The mobile phase consisted of 25 mM ammonium hydroxide ($NH_4OH$) and 25 mM ammonium acetate ($NH_4OAc$) in water (mobile phase A), and acetonitrile (ACN) (mobile phase B). The injection volume was 2 μL per sample. A flow rate of 0.45 mL $min^{-1}$ was used with the following gradient: 0–1 min, 95% B; 1–14 min, 95% to 65% B; 14–16 min, 65% to 40% B; 16–18 min, 40% B; 18–18.1 min, 40% to 95% B; 18.1–23 min, 95% B. Mass spectra were acquired using a Dual Agilent Jet Stream (AJS) electrospray ionization (ESI) source in positive ion mode. Data were collected in profile mode over an $m/z$ range of 50–1200. MS/MS spectra were collected *via* data-dependent acquisition (DDA) mode.

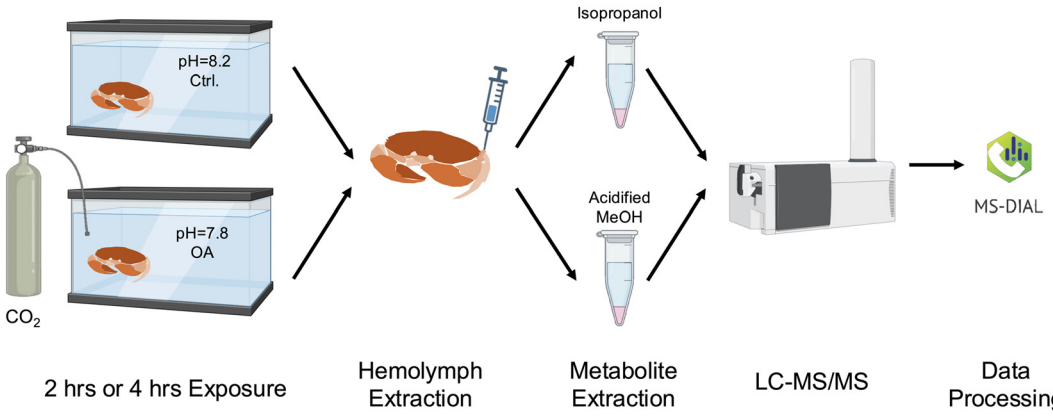


**Fig. 1** Schematic illustrating the workflow of metabolomic profiling of Jonah crabs under OA, coupled with HPLC-QToF mass spectrometry.



### Data analysis

The raw mass spectra were initially processed and analyzed using Agilent MassHunter Qualitative Analysis 10.0. Subsequent peak detection and metabolite annotation were performed with MS-DIAL 4.90 software.[29] MS-DIAL software, which supports various platforms including LC/MS, LC-MS/MS, GC/MS, and GC-MS/MS, was employed due to its robust workflow that integrates raw data processing, peak detection, identification, and statistical analysis. Peak areas were normalized to the Total Ion Chromatogram (TIC) values to minimize inter-sample variability in signal intensity and ensure comparability across samples. The quantification was based on peak area. Normalized data were then filtered on Microsoft Excel primarily and further analyzed using Python-based statistical packages. Compounds were analyzed based on their InChIKey identifier. For the OA exposure experiment, quantitative differences between treatment groups were evaluated using Welch's two-tailed *t*-test to compare each treatment group against the control.

## Results and discussion

### Metabolite identification and metabolome composition

To annotate the acquired mass spectral peaks, the ESI(+)-MS/MS library (standards + biological + *in silico*) from the metabolomics reference database was selected in MS-DIAL, as it is well-suited for positive-mode metabolomics of biological samples. During data processing, the mass tolerance was set to 0.05 Da for MS1 and 0.1 Da for MS2. Identified peaks were screened based on the following criteria: a signal-to-noise ratio greater than 5, a mass error below 20 ppm, and a match with the MS-DIAL reference library.

The IPA-extracted control group was used to establish a reference metabolomic profile under normal seawater conditions, as this method provides broader metabolite coverage, which is demonstrated in the subsequent section. In the IPA control group, a total of 3 599 ± 322 (mean ± SD) spectral features were initially detected (averaged across five biological replicates). After applying identification and filtering criteria, 324 compounds remained in the final annotated list. For high-throughput classification, annotated compounds were mapped to Human Metabolome Database (HMDB) IDs and matched against the comprehensive HMDB dataset.[30] Although HMDB database is not designed for crustacean metabolomics, it provides the most extensive support for compound classification among currently available databases. The complete list of classified metabolites is provided in Table S1. The compositional distribution of the annotated metabolites is shown in Fig. 2, revealing a significant proportion of organoheterocyclic compounds (21.8%), lipids and lipid-like molecules (19.1%), amino acids, peptides, and analogues (16.4%).

The predominance of organoheterocyclic compounds in the metabolite profile likely reflects the structural diversity of small molecules involved in essential biological functions such as signalling, osmoregulation, and detoxification in marine crustaceans.[31] A large proportion of the lipids detected in the hemolymph were glycerophospholipids and fatty acids. Glycerophospholipids serve as essential components of cellular membranes and are involved in maintaining membrane structure, signalling, and transport functions.[32] The presence of fatty acids, which likely serve as energy sources or signalling molecules, reflects energy metabolism and physiological state.[33,34] These observations establish a reference metabolic profile under normal seawater conditions.

### Comparative analysis of IPA and AcMeOH metabolite extraction methods

In metabolomics, PPT is a crucial step for removing high-abundance proteins that can interfere with the detection and quantification of metabolites. Currently, organic-solvent-induced protein PPT and ultrafiltration are two of the most widely used methods.[35] PPT offers several advantages over other extraction methods, including operational simplicity, effective protein removal, broad metabolite coverage, and reduced metabolite loss.[35,36] Acidified methanol has long been an important extraction solvent in both metabolomics and peptidomics.[37–39] Isopropanol is a commonly used protic

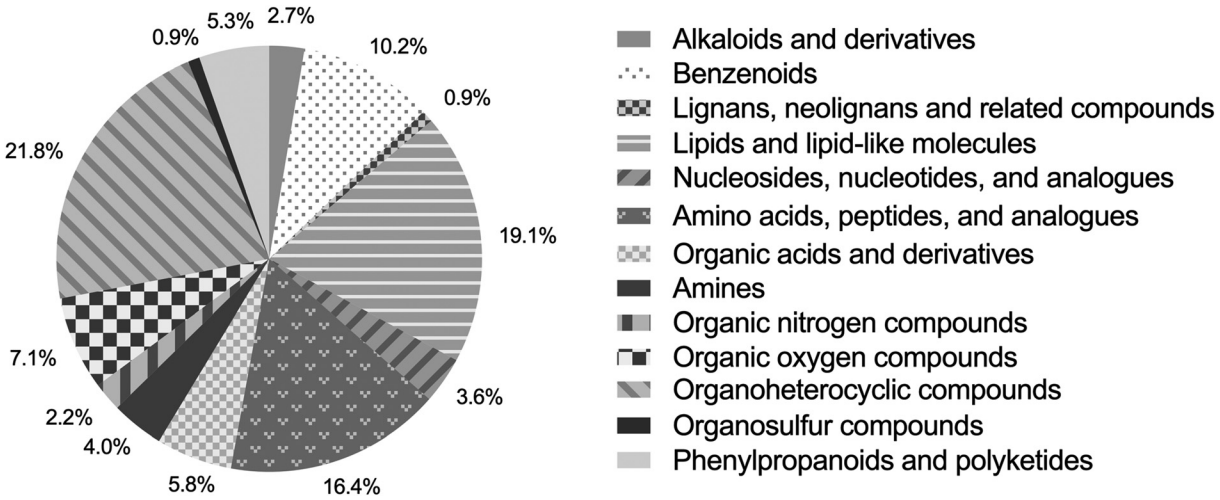


**Fig. 2** Chemical classification of annotated metabolites. The pie chart illustrates the distribution of metabolites in the IPA control group (pH 8.2, $n$ = 5). The proportions of chemical classes are labeled alongside each segment of the chart.

solvent known for its ability to induce protein denaturation and precipitation. It has proven useful in metabolomics studies due to its capacity to extract a wide range of metabolites.[40–42]

To achieve a more comprehensive profile of the Jonah crab metabolome for OA experiments, we compared the metabolite extraction efficiency of IPA and AcMeOH in the control group. As shown in Fig. 3a, IPA extraction yielded 676 compounds, while AcMeOH extraction yielded 496, with an overlap of 203 compounds between the two methods. The complete lists of classified metabolites are provided in Tables S1 and S2. The precursor ion $m/z$ distribution (Fig. 3b) shows that the IPA method covered more compounds with higher $m/z$ values compared to AcMeOH. Among the annotated metabolite classes (Fig. 3c), IPA extraction yielded slightly more organoheterocyclic compounds (49 compared to 42 with AcMeOH) and significantly more lipids (43 compared to 15 with AcMeOH), with notable enrichment in glycerophospholipids and steroids. Glycerophospholipids were nearly absent in the AcMeOH group, suggesting that this solvent system is inefficient for extracting such lipid species. This likely contributes to the overall higher number of metabolites observed in the IPA group. For other metabolite classes, including nucleosides and nucleotides (10 with AcMeOH compared to 8 with IPA) as well as amino acids and peptides (40 with AcMeOH compared to 37 with IPA), only minor differences in compound counts were observed between the two extraction methods.

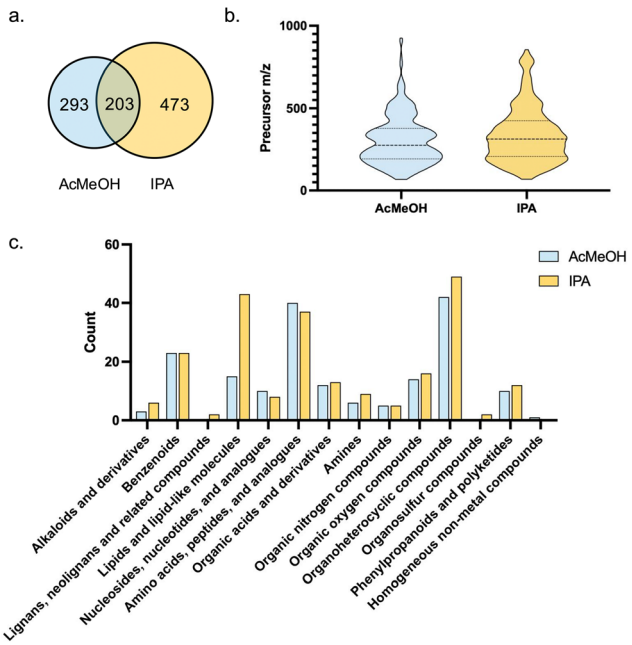


**Fig. 3** Comparison of metabolite extraction efficiency between IPA and AcMeOH in the control group. (a) Venn diagram showing the total number of compounds extracted by IPA and AcMeOH, including the number of shared and unique compounds between the two methods. (b) Distribution of precursor ion $m/z$ values for compounds extracted by each method, showing that IPA covered a broader and higher $m/z$ range. (c) Chemical class distribution of annotated metabolites based on HMDB classification.

### Optimization of OA exposure experiment and metabolite extraction methods

Untargeted metabolomics was first conducted on hemolymph samples extracted from crabs after 2 hour and 4 hour exposure to acidified seawater, using IPA as the primary extraction solvent. Each group consisted of five biological replicates. In the control group, crabs were incubated in standard seawater (pH 8.2), while the OA groups were exposed to acidified seawater (pH 7.8) for 2 or 4 hours. After metabolite extraction with IPA, we compared the numbers of upregulated and downregulated compounds between the control and treatment groups. In the comparison of the 2 hour OA exposure group and the control group (Fig. 4a), we identified three signifi-

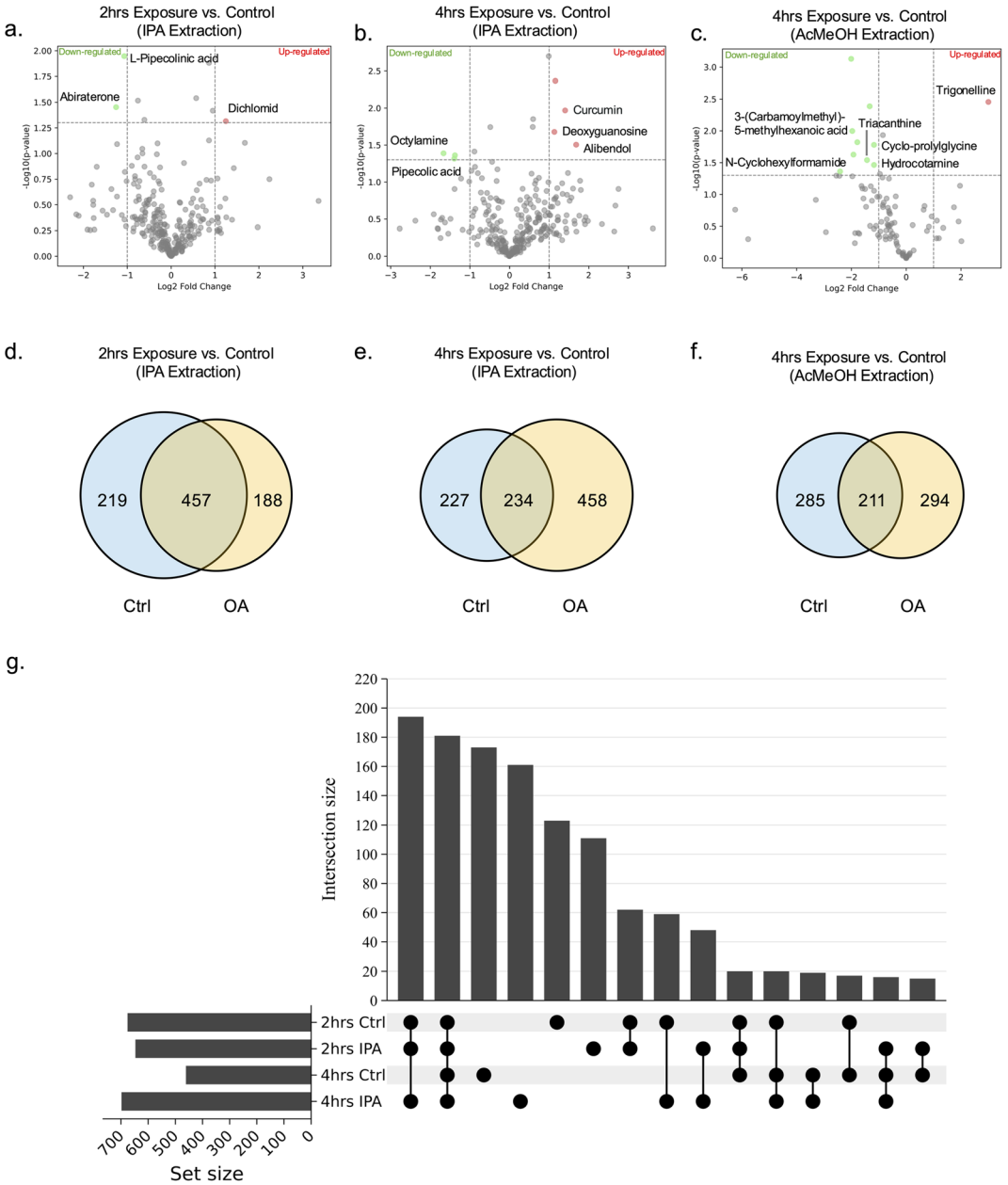


**Fig. 4** Differential metabolite analysis in Jonah crab hemolymph following 2 and 4 hour OA exposures. (a) Significantly altered metabolites ($p$ < 0.05, FC > 2) extracted by IPA, comparing the 2 hour control and 2 hour OA exposure groups. (b) Comparison between the 4 hour control and 2 hour OA exposure groups using IPA extraction. (c) Comparison between the 4 hour control and 4 hour OA exposure groups using AcMeOH extraction. (d–f) Venn diagrams showing the total number of compounds detected in the control and OA groups, including shared and unique compounds between the two extraction methods. (g) UpSet plot illustrating the overlap and condition-specific metabolite features among different experimental groups, generated using ChiPlot (https://www.chiplot.online/).

cantly regulated metabolites, indicating a response to OA treatment. However, the limited number of affected metabolites was insufficient to suggest a robust or broad-scale metabolic alteration. Notably, the 4 hour exposure group exhibited significantly more altered metabolites than the 2 hour group, as shown in Fig. 4a and b, suggesting enhanced metabolic changes with prolonged exposure. In our earlier comparison of extraction efficiency, IPA yielded a higher number of total compounds compared to AcMeOH. However, AcMeOH still provided 293 unique compound IDs not captured by IPA, indicating complementary extraction profiles. Based on these findings, the 4 hour exposure condition was selected for further study. Both IPA and AcMeOH extraction methods were applied in parallel, and the results were integrated for downstream analysis to ensure broader metabolite coverage.

### Metabolite analysis in OA exposure experiment

The Jonah crab has been extensively studied for its adaptations to various stress conditions, including fasting, hypoxia, and temperature fluctuations, and is known to exhibit flexible and dynamic changes at the proteomic level.[28,43–45] Building on the optimization result described above, we analyzed the metabolomic alterations from the 4 hour OA exposure experiment. The complete list of detected metabolites is provided in Tables S3–S6. The extracted metabolite lists were screened and statistically analyzed using Welch's two-tailed *t*-tests, and metabolites exhibiting $p$ values <0.05 were considered significantly altered. In the volcano plots of the 4 hour exposure groups (Fig. 4a–c), we identified 4 upregulated and 3 downregulated metabolites in the IPA extraction dataset, and 1 upregulated and 9 downregulated metabolites in the AcMeOH extraction dataset. Several of these metabolites have been previously reported in related studies and are labelled in Fig. 4, while others remain poorly characterized in the current literature. The abundance changes of these metabolites are shown in Fig. 5, and their molecular structures and PubChem CIDs are presented in Fig. S1. The information for these metabolites is provided in Table 1. Among the annotated metabolites, curcumin (upregulated, FC = 2.64, $p$ = 0.0107), deoxyguanosine (upregulated, FC = 2.19, $p$ = 0.0210), trigonelline (upregulated, FC = 8.00, $p$ = 0.0035), pipecolic acid (downregulated, FC = 2.63, $p$ = 0.0483), and cycloprolylglycine (downregulated, FC = 2.26, $p$ = 0.0166) have been previously reported in association with marine animals or marine-derived organisms. Fold change (FC) represents the ratio of mean metabolite abundance between the 4 hour OA group and control group. In contrast, other compounds including octylamine (downregulated, FC = 3.17, $p$ = 0.0409), alibendol (upregulated, FC = 3.21, $p$ = 0.0312), *N*-cyclohexylformamide (downregulated, FC = 3.80, $p$ = 0.0237), deoxyguanosine (upregulated, FC = 2.19, $p$ = 0.0210), triacanthine (downregulated, FC = 2.70, $p$ = 0.0288), and hydrocotarnine (downregulated, FC = 2.26, $p$ = 0.0344) show no clear evidence of connection to marine organisms based on current literature. We also observed notable variation in feature presence and absence across different OA exposure times. Venn diagrams and UpSet plots (Fig. 4d–g) show that the IPA-extracted 2 hour OA group contains 188 uniquely detected metabolite features, whereas the 4 hour OA group contains 458 unique features.

To further explore the potential physiological relevance of these metabolites, we examined their known functions and possible origins. Cycloprolylglycine (downregulated, FC = 2.26, $p$ = 0.0166) is an endogenous neuropeptide identified in the rat brain,[46] exhibits a wide range of biological activities, including nootropic, antihypoxic, neuroprotective, and anxiolytic effects.[47] It functions as a positive modulator of AMPA receptors, and its anxiolytic and antihypoxic effects have been shown to depend on BDNF/Trk signalling.[48,49] Although there is no direct evidence of cycloprolylglycine in marine species, indirect evidence suggests it can be processed in the mouse brain following gavage with tilapia head protein hydrolysate, indicating a potential link to marine-derived precursors.[50] Given the high peak area of cycloprolylglycine detected in our dataset and the lack of microbial origin reports, it is plausible that cycloprolylglycine may represent a previously unreported endogenous metabolite in Jonah crabs. Its observed downregulation under OA conditions may reflect increased utilization in response to environmental stress. Curcumin (upregulated, FC = 2.64, $p$ = 0.0107), a turmeric-derived compound, is widely studied for its benefits in marine species and is increasingly used as a feed additive in aquaculture.[51] In greater amberjack (*Seriola dumerili*), it enhances antioxidant-related gene expression and enzyme activity by upregulating glutathione

**Table 1** Significantly regulated metabolites identified under OA conditions

| Compound name | Molecular formula | Adduct | *m/z* | Ontology | Mass error (ppm) | Retention time (min) |
|---|---|---|---|---|---|---|
| Curcumin | $C_{24}H_{31}NO$ | $[M + NH_4]^+$ | 386.1662 | Androgens and derivatives | 16.5216 | 19.1899 |
| Trigonelline | $C_7H_7NO_2$ | $[M + Na]^+$ | 160.0375 | Alkaloids and derivatives | 3.7491 | 16.1656 |
| Deoxyguanosine | $C_{10}H_{13}N_5O_4$ | $[M + Na]^+$ | 290.0852 | Purine 2′-deoxyribonucleosides | 2.6543 | 11.7049 |
| Alibendol | $C_{13}H_{17}NO_4$ | [M + H]+ | 252.1218 | Salicylamides | 4.8785 | 11.8488 |
| Cycloprolylglycine | $C_7H_{10}N_2O_2$ | $[M + H]^+$ | 155.0798 | Amino acids | 10.9619 | 20.8963 |
| Pipecolic acid | $C_6H_{11}NO_2$ | $[M + H]^+$ | 152.0673 | Alpha amino acids | 5.9841 | 18.8486 |
| Hydrocotarnine | $C_{12}H_{15}NO_3$ | $[M + H]^+$ | 222.1102 | N/A | 10.22 | 9.5753 |
| 5-[(*E*)-3-Hydroxy-3-methylbut-1-enyl]-2-methylcyclohex-5-ene-1,2,4-triol | $C_{12}H_{20}O_4$ | $[M + HN_4]^+$ | 246.1669 | Trialkyl phosphates | 6.6249 | 18.1649 |
| 4,9-Dimethoxy-7-(perfluorobutyl)-5*H*-furo[3,2-*g*]chromen-5-one | $C_{17}H_9F_9O_5$ | $[M + H]^+$ | 465.0391 | Furanochromones | 1.9568 | 11.7029 |
| 2-(4-Aminotetrahydro-2*H*-pyran-4-yl) acetic acid | $C_7H_{13}NO_3$ | $[M + Na]^+$ | 182.0796 | Pyranoid amino acids and derivatives | 2.1968 | 14.7533 |
| 3-(2-Amino-2-oxoethyl)-5-methyl-hexanoic acid | $C_9H_{17}NO_3$ | $[M + Na]^+$ | 210.1105 | Medium-chain fatty acids | 2.0941 | 10.9556 |
| Methyl 2-[(2-hydroxy-3-methylbutanoyl) amino]-3-methylbutanoate | $C_{11}H_{21}NO_4$ | $[M + Na]^+$ | 254.1373 | *N*-Acyl-alpha amino acids and derivatives | 4.0135 | 10.6468 |
| *N*-Cyclohexylformamide | $C_7H_{13}NO$ | $[M + H]^+$ | 128.1058 | Secondary carboxylic acid amides | 9.2891 | 8.3236 |
| Triacanthine | $C_{10}H_{13}N_5$ | $[M + H]^+$ | 204.1313 | 6-Aminopurines | 6.3684 | 19.1649 |
| Octylamine | $C_8H_{19}N$ | $[M + H]^+$ | 130.1581 | Monoalkylamines | 7.1451 | 13.2442 |

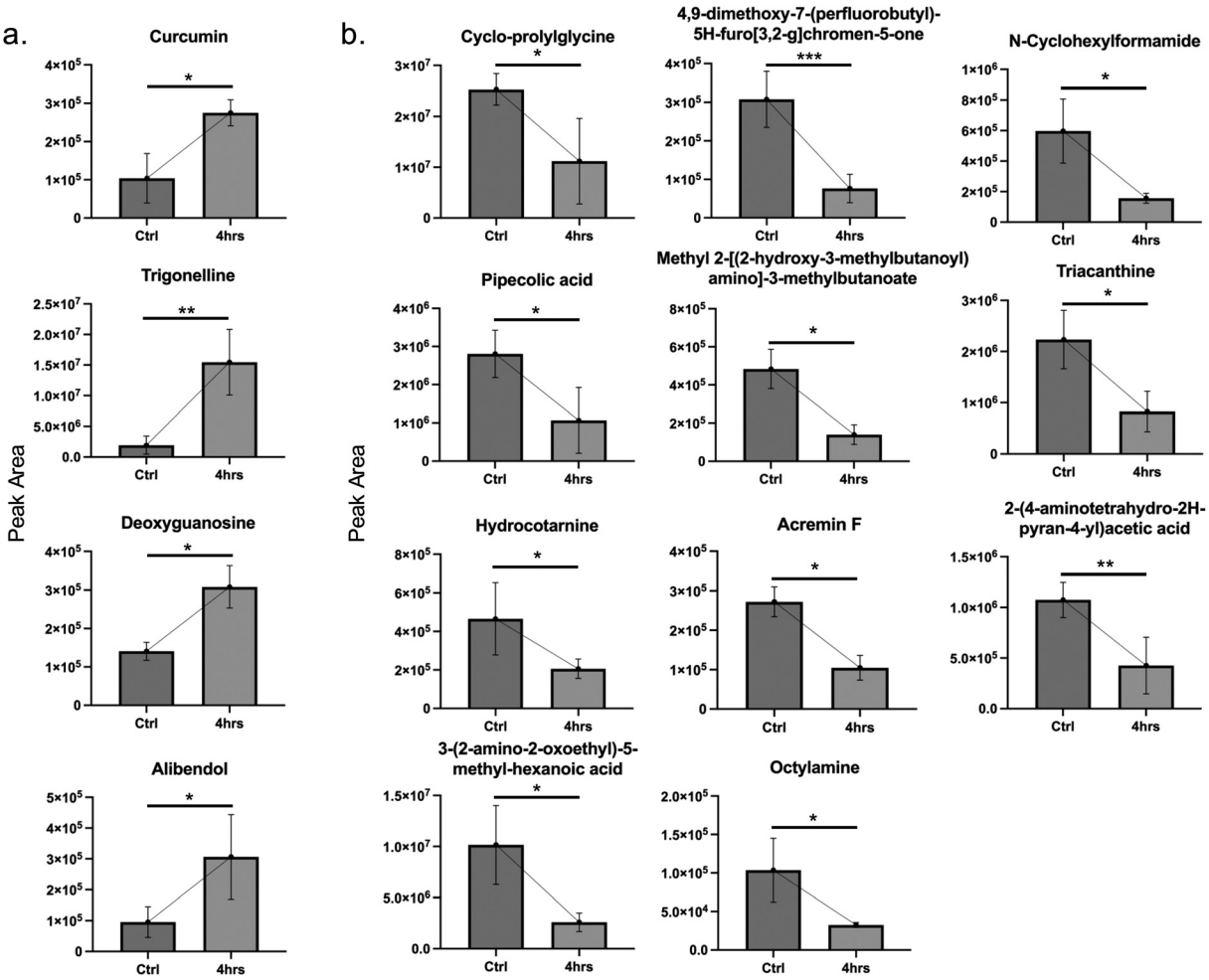


**Fig. 5** Column plots showing the abundance levels of significantly altered metabolites based on peak area. Each column represents the normalized peak area (mean ± SD) of metabolites identified as significantly regulated under OA conditions. Data are shown for both IPA and AcMeOH extraction methods. Statistical significance was determined using an unpaired two-tailed Welch's two-tailed *t*-test. Asterisks indicate levels of significance: *$p < 0.05$, **$p < 0.01$, ***$p < 0.001$. (a) Upregulated metabolites. (b) Downregulated metabolites.

peroxidase and downregulating Keap1 and glutathione reductase, thereby improving the organism's tolerance to environmental stressors.[52] Its presence in crab hemolymph may reflect dietary exposure from prior feeding by the supplier rather than endogenous biosynthesis. Trigonelline (upregulated, FC = 8.00, $p = 0.0035$) is a ubiquitous osmolyte found in various organisms, including reef-building corals[52,53] and algae.[54] It is a metabolite of nicotinamide involved in plant cell cycle regulation and oxidative stress and has been studied through its degradation pathway in corals.[55,56] However, its metabolism in marine animals remains largely unexplored. Pipecolic acid (downregulated, FC = 2.63, $p = 0.0483$) is a naturally occurring non-canonical amino acid present in various organisms, including microorganisms, plants, and animals.[57] It has been detected in the Dungeness crab (*Cancer magister*), although its metabolic role and underlying mechanisms in marine crustaceans remain uncharacterized.[58]

Several other compounds detected in crab hemolymph are not directly associated with marine species. Octylamine (downregulated, FC = 3.17, $p = 0.0409$) is known as an environmental contaminant used in industrial and chemical processes. It has been employed as an extraction agent and is emitted from coatings and polymer formulations, potentially leading to environmental release.[59] Its downregulation may indicate enhanced clearance or transformation of exogenous compounds during physiological stress. Deoxyguanosine (upregulated, FC = 2.19, $p = 0.0210$) was significantly elevated in our dataset. While 8-oxo-deoxyguanosine (8-oxo-dG) is a well-known oxidative stress biomarker,[60] it was not detected in our analysis. The upregulation of deoxyguanosine—a deoxynucleoside with high ionization efficiency in positive mode—may indirectly reflect oxidative stress or DNA damage.[61,62] This observation suggests that oxidative stress-induced DNA degradation may have occurred, with deoxyguanosine being more readily detected under our MS conditions.

Overall, these results highlight the complex biochemical responses of Jonah crabs to short-term OA exposure. The observed changes in both endogenous and exogenous metabolites suggest active molecular adaptations involving anti-

 

oxidant defense and potential DNA repair or degradation processes. The detection of both marine-related and exogenous compounds further underscores the value of hemolymph metabolomics in capturing a broad spectrum of physiological and environmental influences. Despite robust analytical coverage, many detected features could not be confidently annotated, reflecting limitations in current metabolite libraries. As such, the biological significance of many metabolites under OA-induced stress remains unclear and warrants further targeted validation. These findings deepen our understanding of stress-induced metabolic alterations in marine crustaceans and offer candidate biomarkers for future studies on resilience.

## Conclusion

Jonah crab hemolymph represents a rich and complex biological matrix well-suited for investigating physiological responses to environmental stressors. In this study, we employed two protein PPT methods: IPA and AcMeOH extraction, to obtain metabolic snapshots, which were analyzed using untargeted mass spectrometry. Our comparison revealed that IPA extraction yielded a slightly more comprehensive and consistent metabolite profile than AcMeOH, particularly with improved lipid coverage. In the OA experiment, we successfully profiled the hemolymph metabolome of Jonah crabs and observed a dynamic range of metabolic responses between individuals in the OA treatment and control groups. This variability suggests biochemical flexibility in how Jonah crabs respond to environmental changes and provides valuable insight into their physiological adaptations to OA. However, a large portion of the metabolites identified in our study, including many significantly regulated compounds, remain unannotated in current metabolite databases. This lack of annotation limits our ability to fully interpret their functional roles in the stress response and highlights the need for further targeted validation. Despite the starvation of crab in standardized laboratory seawater for one week, we still detected exogenous compounds such as curcumin. This observation highlights the potential influence of prior environmental exposure or dietary history on the metabolome, even under controlled experimental conditions. Future studies on targeted metabolomics combined with classical physiological and biochemical assays, such as measurements of reactive oxygen species (ROS) levels and antioxidant enzyme activities, will be essential to validate the identities of key metabolites and to more directly link observed metabolic changes to oxidative stress and adaptive responses. Together, these findings establish a foundational metabolic profile for Jonah crabs and provide insight into their biochemical plasticity. They also emphasize the challenges and opportunities in advancing metabolite annotation for marine species, which is essential for deepening our understanding of stress-induced metabolic alterations and identifying biomarkers of resilience to OA.

## Author contributions

Y. Y., O. R., L. L. conceived the project and designed the study. Y. Y. performed the experiments, data analysis, and wrote the manuscript. O. R. contributed to experimental procedures. S. X. supervised instrument operation, conducted experiments, and provided revisions to the manuscript. L. L. supervised the project and acquired funding. All authors have read and approved the final manuscript.

## Conflicts of interest

The authors declare no competing financial or non-financial interests.

## Data availability

Due to size and number of raw data files acquired during the preparation of this manuscript, the data will be made available upon request.

Supplementary information (SI): Fig. S1 and Tables S1–S6. See DOI: https://doi.org/10.1039/d5an00788g.

## Acknowledgements

The study was supported in part by a National Science Foundation grant CHE-2108223 and National Institutes of Health grants R01DK071801. Some of the mass spectrometers were acquired using NIH shared instrument grants S10 OD028473, S10 RR029531 and S10 OD025084. S. X. acknowledges the funding support for a Postdoctoral Career Development Award provided by the American Society for Mass Spectrometry. L. L. wishes to acknowledge additional funding support from NIH grants R01AG078794 and R01AG052324, Kellett Mid-Career Award, and the Vilas Distinguished Achievement Professorship, the Charles Melbourne Johnson Professorship, the Wisconsin Alumni Research Foundation, and the University of Wisconsin–Madison School of Pharmacy.

## References

1 L.-Q. Jiang, *et al.*, Global Surface Ocean Acidification Indicators From 1750 to 2100, *J. Adv. Model. Earth Syst.*, 2023, **15**(3), e2022MS003563.
2 J. Gaubert, *et al.*, Impact of ocean acidification on the metabolome of the brown macroalgae Lobophora rosacea from New Caledonia, *Algal Res.*, 2020, **46**, 101783.
3 C. Sanchez-Arcos, *et al.*, Responses of the Macroalga Ulva prolifera Müller to Ocean Acidification Revealed by Complementary NMR- and MS-Based Omics Approaches, *Mar. Drugs*, 2022, **20**, 743, DOI: 10.3390/md20120743.

4 S. Flecha, *et al.*, pH trends and seasonal cycle in the coastal Balearic Sea reconstructed through machine learning, *Sci. Rep.*, 2022, **12**(1), 12956.
5 R. Licker, *et al.*, Attributing ocean acidification to major carbon producers, *Environ. Res. Lett.*, 2019, **14**(12), 124060.
6 C. Mora, *et al.*, Biotic and Human Vulnerability to Projected Changes in Ocean Biogeochemistry over the 21st Century, *PLoS Biol.*, 2013, **11**(10), e1001682.
7 M. R. Miller, *et al.*, Evidence for an effective defence against ocean acidification in the key bioindicator pteropod Limacina helicina, *ICES J. Mar. Sci.*, 2023, **80**(5), 1329–1341.
8 J. C. Orr, *et al.*, Anthropogenic ocean acidification over the twenty-first century and its impact on calcifying organisms, *Nature*, 2005, **437**(7059), 681–686.
9 N. Bednaršek, *et al.*, Limacina helicina shell dissolution as an indicator of declining habitat suitability owing to ocean acidification in the California Current Ecosystem, *Proc. R. Soc. B*, 2014, **281**(1785), 20140123.
10 P. J. Buchanan, *et al.*, Optimization of the World Ocean Model of Biogeochemistry and Trophic dynamics (WOMBAT) using surrogate machine learning methods, *Biogeosciences*, 2025, **22**(19), 5349–5385.
11 P. Thor, *et al.*, Ocean acidification causes fundamental changes in the cellular metabolism of the Arctic copepod Calanus glacialis as detected by metabolomic analysis, *Sci. Rep.*, 2022, **12**(1), 22223.
12 A. Polukhin, The role of river runoff in the Kara Sea surface layer acidification and carbonate system changes, *Environ. Res. Lett.*, 2019, **14**(10), 105007.
13 K. J. Kroeker, *et al.*, Meta-analysis reveals negative yet variable effects of ocean acidification on marine organisms, *Ecol. Lett.*, 2010, **13**(11), 1419–1434.
14 J. P. Gattuso, *et al.*, Effect of calcium carbonate saturation of seawater on coral calcification, *Glob. Planet. Change*, 1998, **18**(1), 37–46.
15 C. Langdon, *et al.*, Effect of calcium carbonate saturation state on the calcification rate of an experimental coral reef, *Global Biogeochem. Cycles*, 2000, **14**(2), 639–654.
16 J. B. Ries, A. L. Cohen and D. C. McCorkle, Marine calcifiers exhibit mixed responses to CO2-induced ocean acidification, *Geology*, 2009, **37**(12), 1131–1134.
17 G. H. Dickinson, *et al.*, Interactive effects of salinity and elevated CO2 levels on juvenile eastern oysters, Crassostrea virginica, *J. Exp. Biol.*, 2012, **215**(1), 29–43.
18 L. F. Dodd, *et al.*, Ocean acidification impairs crab foraging behaviour, *Proc. R. Soc. Lond. B. Biol. Sci.*, 2015, **282**(1810), 20150333.
19 K. S. Longmire, *et al.*, Biological responses of the predatory blue crab and its hard clam prey to ocean acidification and low salinity, *Mar. Ecol. Prog. Ser.*, 2022, **701**, 67–81.
20 D. J. Creek, Stable Isotope Labeled Metabolomics Improves Identification of Novel Metabolites and Pathways, *Bioanalysis*, 2013, **5**(15), 1807–1810.
21 N. W. Snyder, *et al.*, Untargeted Metabolomics from Biological Sources Using Ultraperformance Liquid Chromatography-High Resolution Mass Spectrometry (UPLC-HRMS), *J. Vis. Exp.*, 2013, (75), e50433.
22 N. Vinayavekhin and A. Saghatelian, Untargeted Metabolomics, *Curr. Protoc. Mol. Biol.*, 2010, **90**(1), 30.1.1–30.1.24.
23 B. Greer, *et al.*, Redefining dilute and shoot: The evolution of the technique and its application in the analysis of foods and biological matrices by liquid chromatography mass spectrometry, *TrAC, Trends Anal. Chem.*, 2021, **141**, 116284.
24 J. A. Haley, D. Hampton and E. Marder, Two central pattern generators from the crab, Cancer borealis, respond robustly and differentially to extreme extracellular pH, *eLife*, 2018, **7**, e41877.
25 L. Lewis and J. Ayers, Temperature preference and acclimation in the Jonah Crab, Cancer borealis, *J. Exp. Mar. Bio. Ecol.*, 2014, **455**, 7–13.
26 L. Li, *et al.*, Mass spectrometric investigation of the neuropeptide complement and release in the pericardial organs of the crab, Cancer borealis, *J. Neurochem.*, 2003, **87**(3), 642–656.
27 D. M. Blitz, *et al.*, Distribution and effects of tachykinin-like peptides in the stomatogastric nervous system of the crab, Cancer borealis, *J. Comp. Neurol.*, 1995, **354**(2), 282–294.
28 Y. Liu, *et al.*, Multifaceted Mass Spectrometric Investigation of Neuropeptide Changes in Atlantic Blue Crab, Callinectes sapidus, in Response to Low pH Stress, *J. Proteome Res.*, 2019, **18**(7), 2759–2770.
29 H. Tsugawa, *et al.*, A lipidome atlas in MS-DIAL 4, *Nat. Biotechnol.*, 2020, **38**(10), 1159–1163.
30 D. S. Wishart, *et al.*, HMDB 5.0: the Human Metabolome Database for 2022, *Nucleic Acids Res.*, 2022, **50**(D1), D622–D631.
31 Y. Wu, *et al.*, Effects of Temporary Rearing with Edetate Disodium on Shrimp (Litopenaeus vannamei) Based on UPLC-MS Untargeted Metabolomics, *J. Aquat. Food Prod. Technol.*, 2025, **33**, 806–822.
32 D. Hishikawa, *et al.*, Diversity and function of membrane glycerophospholipids generated by the remodeling pathway in mammalian cells, *J. Lipid Res.*, 2014, **55**(5), 799–807.
33 P. C. Calder, Functional Roles of Fatty Acids and Their Effects on Human Health, *J. Parenter. Enteral. Nutr.*, 2015, **39**(1S), 18S–32S.
34 F. Culkin and R. J. Morris, The fatty acids of some marine crustaceans, *Deep-Sea Res. Oceanogr. Abstr.*, 1969, **16**(2), 109–116.
35 B. Zhang, *et al.*, Nanoparticle-Assisted Removal of Protein in Human Serum for Metabolomics Studies, *Anal. Chem.*, 2016, **88**(1), 1003–1007.
36 K. Contrepois, L. Jiang and M. Snyder, Optimized Analytical Procedures for the Untargeted Metabolomic Profiling of Human Urine and Plasma by Combining Hydrophilic Interaction (HILIC) and Reverse-Phase Liquid Chromatography (RPLC)–Mass Spectrometry*, *Mol. Cell. Proteomics*, 2015, **14**(6), 1684–1695.

 

37 C. Keller, *et al.*, Extraction optimization for combined metabolomics, peptidomics, and proteomics analysis of gut microbiota samples, *J. Mass Spectrom.*, 2021, **56**(4), e4625.
38 Q. Cao, *et al.*, Profiling of small molecule metabolites and neurotransmitters in crustacean hemolymph and neuronal tissues using reversed-phase LC-MS/MS, *Electrophoresis*, 2018, **39**(9–10), 1241–1248.
39 H. Ye, *et al.*, Quantitative Mass Spectrometry Reveals Food Intake-Induced Neuropeptide Level Changes in Rat Brain: Functional Assessment of Selected Neuropeptides as Feeding Regulators, *Mol. Cell. Proteomics*, 2017, **16**(11), 1922–1937.
40 K. Dettmer, *et al.*, Metabolite extraction from adherently growing mammalian cells for metabolomics studies: optimization of harvesting and extraction protocols, *Anal. Bioanal. Chem.*, 2011, **399**(3), 1127–1139.
41 I. Kohler, *et al.*, Hydrophilic interaction chromatography – mass spectrometry for metabolomics and proteomics: state-of-the-art and current trends, *Microchem. J.*, 2022, **175**, 106986.
42 C. Andresen, *et al.*, Comparison of extraction methods for intracellular metabolomics of human tissues, *Front. Mol. Biosci.*, 2022, **9**, 2022.
43 R. Chen, *et al.*, Quantitative Neuropeptidomics Study of the Effects of Temperature Change in the Crab Cancer borealis, *J. Proteome Res.*, 2014, **13**(12), 5767–5776.
44 A. R. Buchberger, *et al.*, Mass Spectrometric Profiling of Neuropeptides in Callinectes sapidus during Hypoxia Stress, *ACS Chem. Neurosci.*, 2020, **11**(19), 3097–3106.
45 K. DeLaney, *et al.*, Mass Spectrometry Quantification, Localization, and Discovery of Feeding-Related Neuropeptides in Cancer borealis, *ACS Chem. Neurosci.*, 2021, **12**(4), 782–798.
46 T. A. Gudasheva, *et al.*, Identification of a novel endogenous memory facilitating cyclic dipeptide cyclo-prolylglycine in rat brain, *FEBS Lett.*, 1996, **391**(1–2), 149–152.
47 T. A. Gudasheva, *et al.*, Anxiolytic Activity of Endogenous Nootropic Dipeptide Cycloprolylglycine in Elevated Plus-Maze Test, *Bull. Exp. Biol. Med.*, 2001, **131**(5), 464–466.
48 T. A. Gudasheva, *et al.*, Neuropeptide cycloprolylglycine increases the levels of brain-derived neurotrophic factor in neuronal cells, *Dokl. Biochem. Biophys.*, 2016, **469**(1), 273–276.
49 T. A. Gudasheva, *et al.*, The Anxiolytic Effect of the Neuropeptide Cycloprolylglycine Is Mediated by AMPA and TrkB Receptors, *Dokl. Biochem. Biophys.*, 2020, **493**(1), 190–192.
50 J. Ji, *et al.*, Synergistic effects of tilapia head protein hydrolysate and walnut protein hydrolysate on the amelioration of cognitive impairment in mice, *J. Sci. Food Agric.*, 2024, **104**(9), 5419–5434.
51 M. S. Fagnon, C. Thorin and S. Calvez, Meta-analysis of dietary supplementation effect of turmeric and curcumin on growth performance in fish, *Rev. Aquacult.*, 2020, **12**(4), 2268–2283.
52 Y. He, *et al.*, Dietary curcumin supplementation can enhance health and resistance to ammonia stress in the greater amberjack (Seriola dumerili), *Front. Mar. Sci.*, 2022, **9**, 2022.
53 R. W. Hill, *et al.*, Abundant betaines in reef-building corals and ecological indicators of a photoprotective role, *Coral Reefs*, 2010, **29**(4), 869–880.
54 G. Blunden, Trigonelline and other betaines in species of Laminariales, *Nat. Prod. Commun.*, 2012, **7**(7), 863–865.
55 N. Perchat, *et al.*, Elucidation of the trigonelline degradation pathway reveals previously undescribed enzymes and metabolites, *Proc. Natl. Acad. Sci. U. S. A.*, 2018, **115**(19), E4358–E4367.
56 M. M. Reddy, *et al.*, Multi-omics determination of metabolome diversity in natural coral populations in the Pacific Ocean, *Commun. Earth Environ.*, 2023, **4**(1), 281.
57 M. Kumari, P. Sharma and A. Singh, Pipecolic acid: A positive regulator of systemic acquired resistance and plant immunity, *Biochim. Biophys. Acta, Gen. Subj.*, 2025, **1869**(7), 130808.
58 S. A. Wanamaker, *et al.*, Uncovering mechanisms of global ocean change effects on the Dungeness crab (Cancer magister) through metabolomics analysis, *Sci. Rep.*, 2019, **9**(1), 10717.
59 U. E. Bollmann, *et al.*, Photodegradation of octylisothiazolinone and semi-field emissions from facade coatings, *Sci. Rep.*, 2017, **7**(1), 41501.
60 J. Y. Hahm, *et al.*, 8-Oxoguanine: from oxidative damage to epigenetic and epitranscriptional modification, *Exp. Mol. Med.*, 2022, **54**(10), 1626–1642.
61 A. P. Null, A. I. Nepomuceno and D. C. Muddiman, Implications of Hydrophobicity and Free Energy of Solvation for Characterization of Nucleic Acids by Electrospray Ionization Mass Spectrometry, *Anal. Chem.*, 2003, **75**(6), 1331–1339.
62 Y. Hua, *et al.*, Comparison of negative and positive ion electrospray tandem mass spectrometry for the liquid chromatography tandem mass spectrometry analysis of oxidized deoxynucleosides, *J. Am. Soc. Mass Spectrom.*, 2001, **12**(1), 80–87.